Mass-Centered Weight Update Scheme for Particle Filter Based Indoor Pedestrian Positioning

Wenhua Shao*, Haiyong Luo†, Fang Zhao*, Cong Wang*, Antonino Crivello‡, Muhammad Zahid Tunio*
* School of Software Engineering, Beijing University of Posts and Telecommunications, Beijing, China
†Institute of Computing Technology, Chinese Academy of Sciences, Beijing, China
‡Institute of Information Science and Technologies, CNR, Italy
‡University of Siena - Department of Information Engineering and Mathematics, Italy
E-mails: {shaowenhua, yhluo}@ict.ac.cn, {zfsse, wangc, zahid.tunio}@bupt.edu.cn, antonino.crivello@isti.cnr.it

***Abstract*—Smartphone based indoor positioning has become a hot topic in pervasive computing, because of the need to improve indoor location-based services. In order to strengthen positioning accuracy, researchers have tried to leverage high-resolution magnetic fingerprint with particle filter and dynamic time warping (DTW). These approaches are computation-hungry, which increases hardware cost for positioning companies. By analyzing magnetic features for pedestrian users, we present a mass-centered weight update scheme to decrease calculation overheads. Finally, the proposed positioning algorithm is tested in a realistic situation, showing high-quality localization capability.**

Keywords—location awareness, indoor positioning, particle filter, magnetic field based positioning

I. INTRODUCTION

The smartphone plays an important role in enabling pervasive computing that facilitates our daily lives. Taking location-based services (LBS) for example, anyone can travel to a new place without bearing any problems with the help of outdoor navigation applications. All these conveniences are supported by global positioning techniques, like GPS, BeiDou, and Galileo. However, walls and ceilings weaken the signals from GPS satellites, so global positioning techniques are only available outdoors.

In order to satisfy indoor LBS requirements, researchers have developed various indoor positioning methods. These techniques include Wi-Fi [1-6] and Bluetooth low energy (BLE) labels [7, 8]. However, because of signal variation, these radio frequency (RF) signal based techniques often suffer from low positioning accuracy. Therefore, it is important to find a new location label that is ubiquitous and with high spatial resolution.

Smartphone-based sensing technologies provide a new approach for indoor positioning. For example, the magnetometer enables a smartphone to sense indoor magnetic field. The inertial measurement unit (IMU) enables a smartphone to detect user's motion and moving orientation. Indoor magnetic fields are pervasive and location related, but its low distinguishability makes it only distinguishable for long motion traces. On the other hand, inertial based methods suffer from drift error gathered during traveling course. For these reasons, current magnetic-based technologies often combine pedestrian dead reckoning (PDR) and magnetic feature fingerprint matching with particle filter techniques [9-15].

Tracking user locations is challenging because the probability distribution of user locations is a mathematical high-dimensional problem. The particle filter is a good choice of processing these issues [16]. Consequently, current works of indoor positioning problems combine particle filter and magnetic fingerprint maps by updating particle weights with the map matching results. In general, matching is evaluated as similarity, but it is difficult to measure the similarity metric between two warping fingerprints. Therefore, researchers use DTW algorithm to measure the likeness between training and positioning fingerprints [10, 11]. Unfortunately, DTW based positioning algorithms are computation hungry, especially when they are applied with large amounts of particles.

The battery capacity of the smartphone is limited, so in order to reduce smartphone power consumption and guarantee strong performances, indoor positioning providers tend to adopt client/server mode. The client, composed by the smartphone, only collects environment signals. Then using an external server, complicated positioning algorithms are evaluated. Using the traditional computation-hungry algorithms—in order to serve mass users—companies and industries should spend more hardware cost for realizing efficient indoor positioning services.

This paper presents a low-cost high-precision fusion positioning system. It combines the advantage of Wi-Fi/BLE and magnetic positioning using Wi-Fi/BLE to initialize a rough position, then a magnetic positioning method based on particle filter is developed to improve positioning accuracy. The core part of this magnetic particle filter algorithm is a mass-centered weight update scheme. The proposed scheme is much computation-efficient than the traditional DTW based methods and still keeps high positioning accuracy.

The major contributions of this work include: i) introducing magnetic field fingerprint features of pedestrian behavior; ii) presenting a low-cost high-accuracy magnetic matching scheme.

The plan of the rest of the paper is as follows: Section II analyses the positioning related features of the indoor magnetic field. Section III presents the proposed positioning solution. It first introduces the system architecture and workflow, then introduces the magnetic features of pedestrian behavior and presents the mass-centered weight update scheme for pedestrians. Section IV extensively evaluates the proposed scheme. Finally, section V discusses results of the proposed work.

II. MAGNETIC FIELD FEATURES

Geomagnetic fields keep static in years [17] and, considering indoor environments, buildings' steel structures steadily warp indoor geomagnetic field patterns [9, 18]. These ferromagnetic structures and furniture warp magnetic fields at different locations, but these warping patterns remain static. Considering our testbed scenario, Figure 1 reveals a strength comparison between two magnetic fingerprints, gathered at different times from the same corridor at a uniform speed (~1m/s). Into a small area, the geomagnetic field strength is supposed to be a static value. On the contrary, values vary a lot from one location to another. This behavior is due to the presence of large ferromagnetic materials including pillars and large iron cabinets, which warp the earth magnetic field. In contrast, small ferromagnetic materials like key chains, coins, and chairs have little influence to it [10]. It is worth to observe an offset between the two fingerprint datasets, simply due to the calibration routine of the magnetometer, which adds a random offset to its measurements [19].

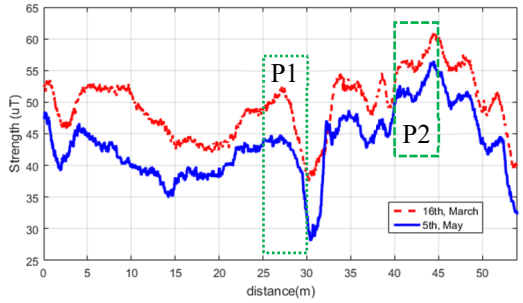

Figure 1. Strength comparison of indoor magnetic fingerprints gathered along a 55 meters long corridor.

Indoor magnetic fields are separable. As Figure 1 reveals, considering lengths of fingerprint segment of 5 meters, the fingerprint pattern of position P1 is different from P2. Therefore, positions can be distinguished by observing indoor magnetic field patterns.

The distinguishability of indoor magnetic fields begins to fade as positioning area enlarges. According to [20], the strength of geomagnetic fields ranges from 25 to 65 μT all over the world. This narrow band is also the rough range of indoor magnetic fields, so it is very crowded for all indoor magnetic fields. Moreover, for consumptive smartphones, the standard deviation of magnetometer noise is around 1 μT [19], which further weakens magnetic field distinguishability.

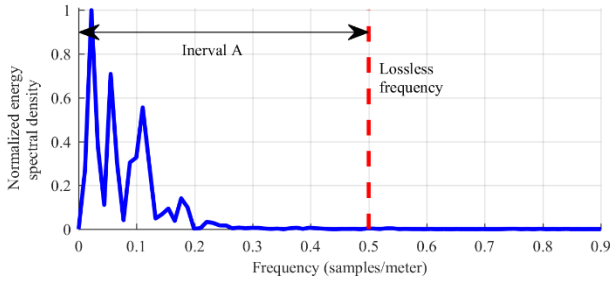

Figure 2. Energy spectral analysis of the indoor magnetic field in the space domain. The result is based on magnetic fingerprints of a whole floor.

The indoor magnetic field is a low-frequency signal in the space domain. As Figure 2 reveals, the main energy of indoor magnetic fingerprints lies in interval A, that is, more than 99% signal energy lies below 0.5 samples/meter. Therefore, we define 0.5 samples/meter as lossless frequency. It is worth mentioning that the pedestrian step frequency is around 1.53 samples/meter [21], so its Nyquist frequency [22] is 0.765 samples/meter, which is greater than the lossless frequency.

III. THE PROPOSED SOLUTION

This section explains the proposed weight update scheme in detail. Part A introduces the system's architecture and explains how it works. Then, part B presents the workflow of the proposed system showing pseudo-code. Successively, part C analyses the magnetic positioning features of pedestrian behaviors, which is the base model of the proposed scheme. Finally, part D proposes the weight update method based on the model described in the previous part.

A. System Architecture

As Figure 3 shows, the proposed smartphone-based positioning system adopts client/server (C/S) architecture. The positioning server contains the positioning algorithm and relative metadata including floor plans, magnetic fingerprints, and Wi-Fi/BLE fingerprints. The smartphone client identifies user steps then sends collected motion and environment signals to the positioning server, and finally, the server calculates real-time positioning results.

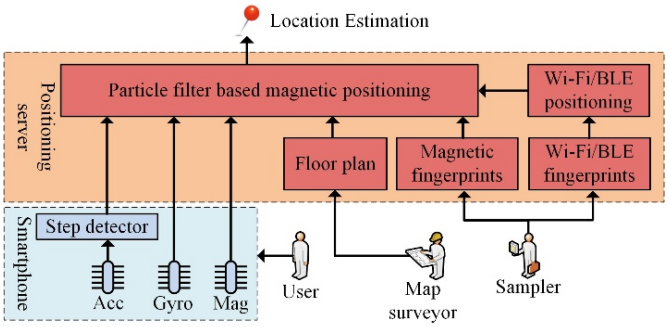

Figure 3. Indoor positioning system architecture. In the smartphone module, Acc means a triaxial accelerometer, Gyro means a triaxial gyroscope, Mag means a triaxial magnetometer. In the positioning system module, BLE means Bluetooth low energy.

Three steps are required to use the system in a real indoor environment: sampling, training, and positioning. During the sampling phase, a user—called a sampler—collects magnetic-field/Wi-Fi/BLE signals of target floors to generate positioning fingerprints; map surveyors survey the floor plans using an AutoCAD software to identify reachable areas for users. Successively, a training phase is performed training magnetic-field/Wi-Fi/BLE models using the dataset collected previously during the sampling phase. Finally, in the positioning phase, users carry smartphones to collect real-time magnetic-field/Wi-Fi/Bluetooth data. When a step detector detects a step event, positioning algorithm estimates a location based on received sensor data, fingerprints, and floor plans.

B. Indoor Positioning Algorithm

Algorithm 1 shows the workflow of the proposed positioning system. It leverages Wi-Fi/Bluetooth positioning module to initialize buildings, floors, and rough location estimations. Successively, with an augmented particle filter, magnetic field fingerprints and user motions are involved, with the purpose of improving positioning accuracy.

The particle filter is an important technique for magnetic positioning, on the contrary, the proposed mass-centered weight update scheme is the key step in the particle filter. The basic idea of the particle filter, also known as Monte Carlo methodology [23], is to use discrete random particles (measures) to approximate the probability of distributions. In the proposed system, each particle is represented as a triplet containing coordinates (x_i, y_i) and a weight ω_i. There are three steps in a particle filter: particle movement, weight update, and particle resampling. In the particle movement step, given a real-time orientation measurement θ, the filter decides the moving direction for each particle with θ and a random variable Δ, with the purpose of enhancing particle diversity. Similarly, the moving distance for each particle is the mean step length S plus a random variable δ. Besides, particles outside reachable areas are removed according to the floor plan. Successively, in the weight update step, the algorithm updates previous particle weights with the mass-centered scheme, according to real-time magnetic fingerprints. The scheme takes into account of all the particles from p_1 to p_N, and their whole history from p_i^1 to p_i^{t-1}, in other words, this update can be expressed as a function $\omega_i^t = f(\ p_1^{t-1}, \cdots,\ p_N^{t-1}, \cdots,\ p_1^1, \cdots,\ p_N^1)$. Further details about the weight update scheme will be explained in the following parts. Finally, the system resamples particles with systematic method [24], and the center of all the resampled particles is calculated as the positioning result.

Algorithm 1 Indoor Positioning Workflow

1: ***Initialization***
2: Wi-Fi/Bluetooth positioning module initializes location l.
3: Randomly spread N particles around l, particle $p_i = (x_i, y_i, \omega_i)$.
4: ***Particle Filter Loop***
5: **while** True **do**
6: **if** detect a step event **then**
Particle Movement
7: $(x_i^t, y_i^t) = (S+\delta)(x_i^{t-1}, y_i^{t-1}) \begin{bmatrix} \cos(\theta+\Delta) & 0 \\ 0 & sin(\theta+\Delta) \end{bmatrix}$.
8: Remove particles outside reachable areas.
9: ***Particle Weight Update by the Mass-Centered Scheme***
$\omega_i^t = f(\ p_1^{t-1}, \cdots,\ p_N^{t-1}, \cdots,\ p_1^1, \cdots,\ p_N^1)$.
10: ***Particle Resample***
Resample particles with systematic resampling [24].
11: Calculate positioning result. $(\widehat{x^t}, \widehat{y^t}) = \frac{1}{N}\sum_N (x_i^t, y_i^t)$.
12: **end if**
13: **end while**

C. Pedestrian Based Magnetic Positioning Features

The weight update method of particles works by comparing the positioning magnetic fingerprints with training fingerprints. As the sixth and seventh lines in Algorithm 1 depicts, a particle moves when a step event is detected. We define the error metric between the true position and a particle position as a particle positioning error (PE). Similarly, we define the magnetic strength error (MSE), which is the error metric between a measured magnetic strength delta and a particle's delta, as Figure 4 shows. From the view of information theory, because the Nyquist frequency of the pedestrian sampling rate is greater than the indoor magnetic lossless frequency, the proposed MSE will retain most indoor magnetic positioning information.

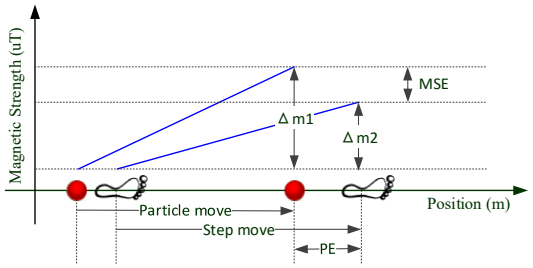

Figure 4. Illustration of a particle positioning error (PE) and a magnetic strength error (MSE).

Considering several steps, we define the mean of PEs as MPE and the mean of absolute MSEs as MMSE. Given N particles and a sliding step window with W steps, for each particle i, its MPE and MMSE at step t are described as:

$$\mathrm{MPE}(i,t) = \frac{1}{W}\sum_{j=0}^{W}\sqrt{(x_i^{t-j} - x_{True}^{t-j})^2 + (y_i^{t-j} - y_{True}^{t-j})^2} \quad \text{(a)}$$

$$\mathrm{MMSE}(i,t) = \frac{1}{W}\sum_{j=0}^{W}\left|\left|s_i^{t-j} - s_i^{t-j-1}\right| - \left|s_{obs}^{t-j} - s_{obs}^{t-j-1}\right|\right| \quad \text{(b)}$$

In the formula (a), (x_i^{t-j}, y_i^{t-j}) represents the position of particle i at step $t-j$. Similarly, $(x_{True}^{t-j}, y_{True}^{t-j})$ stands for the ground truth of users. Then the MPE of particle i is the average of all PEs within the sliding window. The function of this sliding window is to adjust the length of history adopted in the system. In the formula (b), $\left|s_i^{t-j} - s_i^{t-j-1}\right|$ is the absolute value of the particle strength delta of particle i moving from step $t-j-1$ to $t-j$. The particle magnetic strength is loaded from training magnetic fingerprint according to the positions of particles. Likewise, the magnetic strength delta of real-time observations is represented as $\left|s_{obs}^{t-j} - s_{obs}^{t-j-1}\right|$. Therefore, the MMSE of particle i is the average of all absolute MSEs within the sliding window.

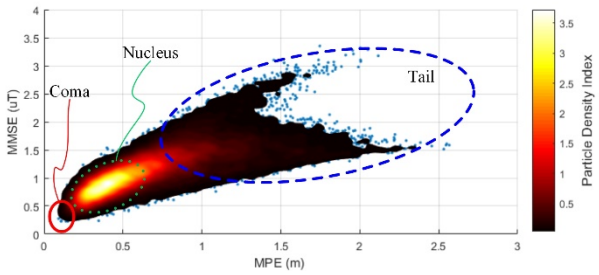

Figure 5. Kernal density estimation of particles. The brighter area stands for higher particle density. The relation comet is drawn with nine steps sliding window.

The relationship between MPE and MMSE can be represented as a comet, shown in Figure 5 with the help of kernel density analysis. The relation comet consists of three parts: nucleus, coma, and tail. The nucleus is the highest density area containing most of the particles. Because the particle movement

model follows a normal distribution, the nucleus gathers most particles around the mean step length. Therefore, the high-density nucleus decides localization results. Successively, particles in the coma are 'valuable' particles, because their MPEs are small, in other words closing to the ground truth. It is worth noticing that these small MPE particles have small MMSE as well. Considering the availability of MMSE and the unavailability of MPE in the positioning phase, the paper presents the scheme that selecting small MPE particles via small MMSE indexes, which will be detailed in part D. Finally, large MPE particles form a diverging tail, because randomly generated step lengths of them are far away from the true step length, either too big or too small.

D. Weight Update Method

In the mass-centered weight update method, step events, floor plans, and magnetic fingerprints are fundamental system inputs. The step events move particles with Markov chain Monte Carlo (MCMC) method. In other words, this method produces a high dimensional particle distribution of possible positions based on dead reckoning and floor plan constriction [16]. The motion model moves particles roughly along user direction, which tunes the distribution of positioning results to fit user motion traces. The floor plan checks particles position and removes those deviated from reachable areas, because, for example, users have no possibility to walk through a wall.

The mass-centered weight update method further improves positioning accuracy by adjusting the weights of particles, based on their similarities between training and positioning magnetic fingerprints. Intuitively, as shown in Figure 5, increasing the weights of coma particles will decrease positioning error. In other words, we can improve positioning accuracy by tuning the comet nucleus towards the coma. Based on this principle, the paper presents the mass-centered weight update method for pedestrian-based magnetic-positioning particle filters. The basic idea of this scheme is increasing the weight of particles with small MMSE, so the paper expresses the weight update scheme with the following formula:

$$\omega_i^t = \begin{cases} K \cdot \frac{\omega_i^{t-1}}{\mathrm{MMSE}(i,t)} & \mathrm{MMSE}(i,t) \geq T \\ K \cdot \frac{\omega_i^{t-1}}{T} & otherwise \end{cases} \quad (c)$$

As shown in formula (c), given N particles, the weight ω_i^t of particle i at step t can be derived from the weight of last step ω_i^{t-1} and the real-time $\mathrm{MMSE}(i,t)$ of this particle. The scheme leverages the reciprocal of $\mathrm{MMSE}(i,t)$ to award the particles with small MMSEs. The weight award is controlled by the parameter K, which is an experimental constant influenced by the sliding window length of the W. In order to prevent particle degeneracy caused by outlier particles [23], the scheme divides the weight update formula into two conditional branches. When $\mathrm{MMSE}(i,t)$ is greater than a threshold T, the scheme updates particle weights following the abovementioned rules. Otherwise, the scheme updates weights with a constant $\frac{K}{T}$. In other words, this threshold set a maximum award for weight update to prevent particle degeneracy. For example, if the $\mathrm{MMSE}(i,t)$ of a particle is infinitesimal, then the weight of this particle will become infinite, causing the extinction all other particles in the filter resampling phase. Parameter T is also an experimental constant influenced by the sliding window length W.

IV. Experiments

This section exhibits the performance of the mass-centered weight update method in a workplace scenario. The section starts with a description of the experimental environments and an instrument specification. Because the key parameters of the mass-centered scheme are experimental constants, the section then conducts evaluations on them. Finally, a performance comparison with traditional positioning techniques is discussed.

A. Instrument Specifications and Experiment Scenario

Experiments collect indoor magnetic data with two commercially available smartphones, specifications shown in Table 1. The smartphones send collected data to a PC server to calculate positioning results. The server equipped with an Intel i5 dual-core CPU and a 16G RAM.

Table 1. Experiment Smartphones

Manufacturer	HTC	Huawei
Phone Series	One X	Mate7
CPU	1.5G, 4 core	1.8G, 4 core
RAM	1GB	3GB

We have conducted the experiments on the seventh floor of an office building. The testbed covers an area of $60m \times 40m$, with a ceiling of $3m$ high. There are many workstations in the middle of the floor and some rooms too, as Figure 6 reveals. Furthermore, along corridors, there are some big metal cabinets, which are helpful in improving positioning accuracy.

Figure 6. A floor plan of our experimental office building. There are some file cabinets along corridors. For example, one of them is represented by a green circle.

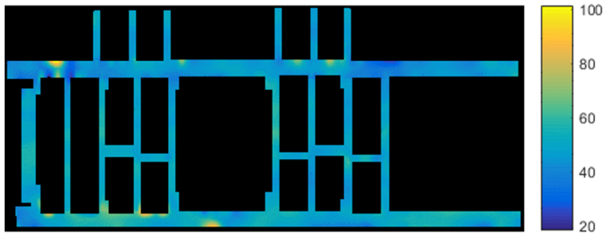

Figure 7. Interpolated magnetic strength map. Different colors represent magnetic strengths, the unit is μT. The black area represents unreachable areas.

Magnetic positioning model: There are two different corridors in our testbed, having 0.7m and 1.6m width respectively. Along narrow corridors, testers collect one sample line along the middle axis of the corridors. Of the wide ones, testers collect another two sample lines parallel with middle axes, with a separation of 0.5m. After data sampling, testers create the magnetic positioning model of the overall testbed with linear

interpolation, as Figure 7 reveals. Positioning fingerprints are collected along randomly selected paths. Every positioning fingerprint is longer than 150 meters. The particle count N is set to 3,000 in this experiment.

B. Key Parameter Evaluations of the Mass-Centered Scheme

Evaluations of sliding window length W: This experiment randomly initializes award parameter K and award threshold parameter T, then increasing the window length W, and observing the change of positioning performance. As Figure 8 reveals, the positioning performance from one step to five steps are approximate and are better than that of six steps and 15 steps, because the longer window length need more particles to cover the increasing diversity. Therefore, with a limited particle population, the performance drops as sliding length enlarges. According to the results, the paper selects the best-performed three steps as the window length for the rest experiments.

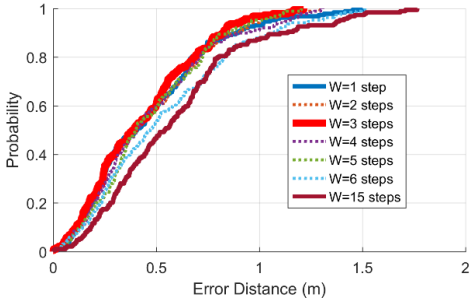

Figure 8. CDFs of different sliding window lengths. Weight award parameters U and threshold parameter T are randomly set to 0.7 and 0.5 respectively. Performances from 1 step to 5 steps are better than that of 6 steps and 15 steps. The three steps window is the best configuration.

Evaluations of award parameter K: Having found a proper sliding window length, this experiment tries to search a good award parameter. The experiment increases award parameter K from a small value to large values, then it compares the performance of the parameters. This experiment evaluates a wide range of K values and draws some typical ones in Figure 9. The result shows that a small award parameter makes the magnetic positioning have little effect on particle weight update, so it is necessary keep award parameter big enough. Experiment results also reveal that too big award parameter have little improvement on the performance too. According to the results, the paper set award parameter K to 70.

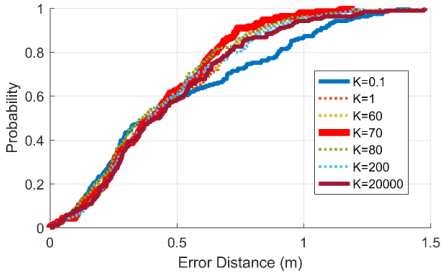

Figure 9. CDFs of different award parameters. The sliding window length is set to three steps according to the previous experiment. The weight threshold parameter T is randomly initialized to 0.5. Performances from K=1 to 20,000 are similar, K=0.1 shows the worst result and K=70 performs the best.

Evaluations of award threshold T: Weight award threshold T is the last parameter to be evaluated after the selection of sliding window length W and the award parameter K. The experiment keeps W and K static, then scanning threshold T and observing its influence to positioning performance, as Figure 10 shows. If the threshold is too big, the selectiveness of the scheme will be weakened, because most of the particles will be awarded with the same weight. In contrast, a too small threshold increases the risk of assigning outlier particles with too big weights, causing particle degeneracy. According to the experiment results, $T = 0.05$ performs the best for the given sliding window length W and the award parameter K.

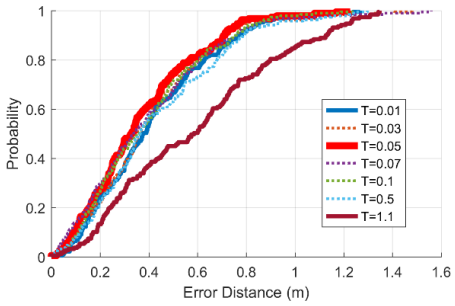

Figure 10. CDFs of different award thresholds. The sliding window length keeps to 3 steps. The weight award parameter K is set to 70 according to the previous experiment. Performances from T=0.01 to 0.5 are similar, T=1.1 shows the worst result and T=0.05 performs the best.

Comparisons with traditional systems: This part compares the performances between the proposed positioning method and traditional methods, with the purpose of revealing the improvement using our approach. As Figure 11 shows, the accuracy of Wi-Fi positioning method is larger than 10 meters at 80%. Using Wi-Fi to provide initial position, the PDR method has little improvement comparing to Wi-Fi only methods, because the distorted indoor magnetic field provides wrong directions for PDR, therefore the PDR performance drops quickly. Floor plan indicates to the system of reachable areas, which improves the performance, because the narrow road restricts the particle divergence, neutralizing compass distortion in some extent. Finally, the experiment adds the magnetic fingerprint to improve accuracy. The paper compares two magnetic fingerprint-matching methods: the proposed mass-centered scheme and the dynamic time warping (DTW) algorithm as implemented in the Magicol system [11]. The performance of the two methods are similar, all of them are less than one meters at the 80%.

The proposed mass-centered scheme is much computationally efficient than the traditional DTW method. As Figure 12 shows, the proposed scheme is 18 times faster than DTW method. When deploying the positioning system on a cloud server, one CPU core can support 130 users considering step period of 0.67 seconds. Therefore, the positioning provider needs two 32-core CPU servers and one 16-core CPU server to support 10,000 users. The monthly hardware budget only needs 2,000 dollars if using the Alibaba cloud-computing platform at US east, saving nearly 30,000 dollars monthly comparing to the DTW method.

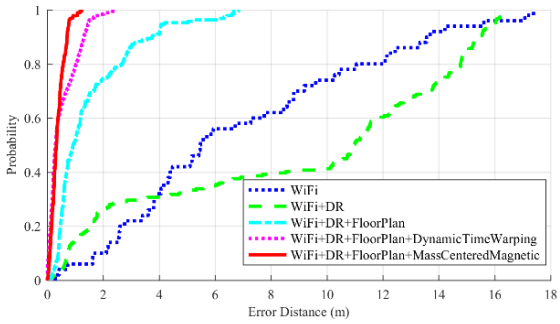

Figure 11. Positioning performance comparison with other systems for moving users. The experiment compares the proposed scheme and other four positioning methods. DR stands for dead reckoning.

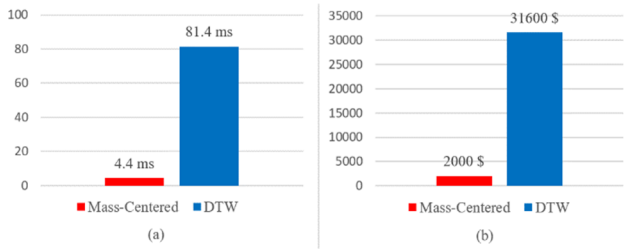

Figure 12. Computation cost comparison between the mass-centered scheme and the DTW method. (a) is the mean computation time. (b) is the monthly hardware budget for 10,000 users.

V. CONCLUSIONS

This paper presents a low-cost mass-centered weight update scheme for particle filter based indoor pedestrian positioning. First, the paper introduces the Wi-Fi/BLE/magnetic fusion positioning system architecture and the fusion-positioning algorithm. The fusion-positioning algorithm utilizes Wi-Fi/BLE to provide initial location, then with a particle filter based magnetic positioning to improve positioning accuracy. Therefore, the paper further introduces the scheme with a magnetic feature analysis and a detailed weight-update method introduction. The proposed mass-centered method is a key step in the particle filter approach, and it guarantees a high accuracy, low cost and low overhead in comparison to classical DTW approach. In the experiments, we also present the evaluation processes of key parameters of our solution.

ACKNOWLEDGMENT

This work was supported in part by the National Key Research and Development Program (2016YFB0502004), the National Natural Science Foundation of China (61374214), the International S&T Cooperation Program of China (2015DFG12520), and the Open Project of the Beijing Key Laboratory of Mobile Computing and Pervasive Device.

REFERENCES

[1] C. Yang and H.-R. Shao, "WiFi-Based Indoor Positioning," *Ieee Communications Magazine,* vol. 53, pp. 150-157, Mar 2015.

[2] X. Xu, L. Xie, and L. Peng, "Design of Indoor Positioning System Based on WiFi Signal Intensity Characteristic," *Computer Engineering,* vol. 41, pp. 87-91, 2015 2015.

[3] Z. Tian, X. Fang, M. Zhou, and L. Li, "Smartphone-Based Indoor Integrated WiFi/MEMS Positioning Algorithm in a Multi-Floor Environment," *Micromachines,* vol. 6, pp. 347-363, Mar 2015.

[4] H. Zou, Y. Zhou, H. Jiang, B. Huang, L. Xie, and C. Spanos, "Adaptive Localization in Dynamic Indoor Environments by Transfer Kernel Learning," in *2017 IEEE Wireless Communications and Networking Conference (WCNC)*, 2017, pp. 1-6.

[5] X. Wang, L. Gao, S. Mao, and S. Pandey, "DeepFi: Deep learning for indoor fingerprinting using channel state information," in *2015 IEEE Wireless Communications and Networking Conference (WCNC)*, 2015, pp. 1666-1671.

[6] F. Potortì, A. Crivello, M. Girolami, E. Traficante, and P. Barsocchi, "Wi-Fi probes as digital crumbs for crowd localisation," in *2016 International Conference on Indoor Positioning and Indoor Navigation (IPIN)*, 2016, pp. 1-8.

[7] Y. Wang, Y. Xu, Z. Yutian, L. Yue, and L. Cuthbert, "Bluetooth positioning using RSSI and triangulation methods," in *2013 IEEE 10th Consumer Communications and Networking Conference (CCNC)*, 2013, pp. 837-842.

[8] J. Hallberg, M. Nilsson, and K. Synnes, "Positioning with Bluetooth," in *10th International Conference on Telecommunications, 2003. ICT 2003.*, 2003, pp. 954-958 vol.2.

[9] E. Le Grand and S. Thrun, *3-Axis magnetic field mapping and fusion for indoor localization*, 2012.

[10] K. P. Subbu, B. Gozick, and R. Dantu, "LocateMe: Magnetic-Fields-Based Indoor Localization Using Smartphones," *Acm Transactions on Intelligent Systems And Technology,* vol. 4, Sep 2013.

[11] Y. Shu, C. Bo, G. Shen, C. Zhao, L. Li, and F. Zhao, "Magicol: Indoor Localization Using Pervasive Magnetic Field and Opportunistic WiFi Sensing," *Ieee Journal on Selected Areas In Communications,* vol. 33, pp. 1443-1457, Jul 2015.

[12] H. Xie, T. Gu, X. Tao, H. Ye, and J. Lv, "MaLoc: A Practical Magnetic Fingerprinting Approach to Indoor Localization using Smartphones," presented at the UBICOMP, SEATTLE, WA, USA, 2014.

[13] H. Xie, T. Gu, X. Tao, H. Ye, and J. Lu, "A Reliability-Augmented Particle Filter for Magnetic Fingerprinting based Indoor Localization on Smartphone," *IEEE Transactions on Mobile Computing,* vol. PP, pp. 1-1, 2015.

[14] X. Guo, W. Shao, F. Zhao, Q. Wang, D. Li, and H. Luo, "WiMag: Multimode Fusion Localization System based on Magnetic/WiFi/PDR," in *Indoor Positioning and Indoor Navigation (IPIN), 2016 International Conference on*, 2016, pp. 1-8.

[15] Q. Wang, H. Luo, F. Zhao, and W. Shao, "An indoor self-localization algorithm using the calibration of the online magnetic fingerprints and indoor landmarks," in *Indoor Positioning and Indoor Navigation (IPIN), 2016 International Conference on*, 2016, pp. 1-8.

[16] K. P. Murphy, *Machine learning: a probabilistic perspective*: MIT press, 2012.

[17] M. McElhinny and P. L. McFadden, *The magnetic field of the earth: paleomagnetism, the core, and the deep mantle* vol. 63: Academic Press, 1998.

[18] M. Angermann, M. Frassl, M. Doniec, B. J. Julian, and P. Robertson, "Characterization of the Indoor Magnetic Field for Applications in Localization and Mapping," *2012 International Conference on Indoor Positioning And Indoor Navigation (Ipin),* 2012 2012.

[19] W. Shao, F. Zhao, C. Wang, H. Luo, T. Muhammad Zahid, Q. Wang, *et al.*, "Location Fingerprint Extraction for Magnetic Field Magnitude Based Indoor Positioning," *Journal of Sensors,* vol. 2016, p. 16, 2016.

[20] A. Wahdan, J. Georgy, and A. Noureldin, "Three-Dimensional Magnetometer Calibration With Small Space Coverage for Pedestrians," *Sensors Journal, IEEE,* vol. 15, pp. 598-609, 2015.

[21] S. H. Shin, C. G. Park, J. W. Kim, H. S. Hong, and J. M. Lee, "Adaptive Step Length Estimation Algorithm Using Low-Cost MEMS Inertial Sensors," in *2007 IEEE Sensors Applications Symposium*, 2007, pp. 1-5.

[22] R. G. Stockwell, L. Mansinha, and R. P. Lowe, "Localization of the complex spectrum: the S transform," *IEEE Transactions on Signal Processing,* vol. 44, pp. 998-1001, 1996.

[23] P. M. Djuric, J. H. Kotecha, J. Zhang, Y. Huang, T. Ghirmai, M. F. Bugallo, *et al.*, "Particle filtering," *IEEE signal processing magazine,* vol. 20, pp. 19-38, 2003.

[24] M. S. Arulampalam, S. Maskell, N. Gordon, and T. Clapp, "A tutorial on particle filters for online nonlinear/non-Gaussian Bayesian tracking," *IEEE Transactions on signal processing,* vol. 50, pp. 174-188, 2002.